Energetically Driven Asymmetries in Random Copolymer Miscibilities and Their Pressure Dependence

Jacek Dudowicz* and Karl F. Freed

The James Franck Institute and the Department of Chemistry, University of Chicago, Chicago, Illinois 60637

Received February 18, 1997; Revised Manuscript Received June 26, 1997[⊗]

ABSTRACT: The extension of random copolymer Flory−Huggins (FH) type theories to compressible systems is applied to describe the miscibilities of $A_xB_{1-x}/C = A,B$ and A_xB_{1-x}/A_yB_{1-y} binary mixtures. The compressible FH type treatment is also generalized to treat lower critical solution temperature phase diagrams. The latter modification involves a model for the leading contribution to the noncombinatorial entropy based on results from the lattice cluster theory for A/B homopolymer blends in which the monomers are assigned specific molecular structures. The blend miscibility gaps, pressure dependence, critical temperature variations, etc. are analyzed and compared with experimental data. In spite of the several noted limitations, the simple theoretical approach qualitatively explains a number of general trends. A more sophisticated molecular theory, which accounts for monomer sequence dependence of the free energy is, however, necessary for the detailed understanding of random copolymer miscibilities.

I. Introduction

The considerable scientific and technological interest in random copolymers arises, in part, from their ability to enhance the mixing of otherwise immiscible systems. This feature may be illustrated by recourse to the properties of a simple blend containing a random copolymer A_xB_{1-x} and a homopolymer C. Assuming the blend is incompressible, the extension of classic Flory−Huggins (FH) theory to random copolymers predicts[1] that the effective interaction parameter χ_{eff} is a weighted average of the individual homopolymer binary interaction parameters χ_{ij}

$$\chi_{\text{eff}} = x\chi_{AC} + (1 - x)\chi_{BC} - x\,(1 - x)\chi_{AB} \qquad (1.1)$$

The interaction parameter χ_{AB} appears in eq 1.1 with a negative sign, thereby promoting blend miscibility for sufficiently "repulsive" A−B interactions. The enormous success of the random copolymer FH type theories in explaining the enhanced miscibilities observed[2,3] for many systems containing random copolymers, as well as in describing[1,2,4,5] some general trends for the phase behavior, has led to the wide spread use of these theories, despite several serious limitations. For example, standard FH theory does not distinguish between systems of block copolymers, random copolymers, alternating copolymers, etc., having identical monomer compositions. Another serious deficiency involves the complete insensitivity of the predicted thermodynamic properties to the pressure and to details of monomer molecular structures, such as their relative sizes and shapes. Polymers processed by extrusion, molding, etc. are subjected to pressures of 10^2−10^3 psi which may affect the blend miscibilities during processing. Hence, treating the polymer systems as incompressible can lead to gross misunderstanding of the phase behavior present in the fabrication process.

One attempt[6] toward improving the FH random copolymer theories retains the simplicity and limitations of the incompressibility assumption, but introduces a physically transparent model for a sequence dependent contribution to the effective interaction parameter χ_{eff}. Our recent extension[7] of the lattice cluster theory[8] (LCT) to treat random copolymer systems provides some insights into the molecular origins of the leading sequence dependent terms in the averaged free energy of random copolymer systems. The leading terms arise from correlations between bonded monomer diads on a single chain and not between triads as previously assumed[6] in the phenomenological model of Balazs *et al.*, which contains six monomer interaction parameters. The evaluation of these terms from the LCT is, however, rather tedious even for the simplest case of a random copolymer melt, and extensive derivations[9] are in progress. Hence, before confronting the full LCT with existing experimental data, it is useful to consider simpler theoretical approaches as a means for separating various physical influences (see below) that are combined together in the more detailed LCT treatment.

A compressible extension of FH theory provides[10] the simplest model for describing influences of "equation-of-state effects" on blend thermodynamic properties. In addition, compressible FH theory plays the role of the zeroth order approximation within the more general LCT. The compressible FH model formalism employs the same basic microscopic parameters as in the LCT, but the former ignores nonrandom mixing contributions that are present in the latter by virtue of chain connectivity, local monomer size disparities, and different monomer−monomer interactions.

Both classic FH theory and its compressible versions assume that the monomers of all polymer species are structureless, uncorrelated entities. Consequently, the noncombinatorial part of the Helmholtz free energy F is represented entirely by the energic contributions which describe the interactions between individual monomers. The treatment of the binary blend as a compressible system implies[10] the presence in a FH type approach of (at minimum) three independent van der Waals attractive energies ϵ_{11}, ϵ_{22}, and ϵ_{12} or, alternatively, three independent macroscopic interaction parameters χ_{ij}. These three interaction parameters contrast sharply with the single χ emerging from classic FH theory. The empirical determination of the three interaction parameters follows the general procedure of mixture theories in which homopolymer parameters χ_{ii} are determined from pure component equation-of-state data, leaving the heterocontact parameter χ_{ij} to be

[⊗] Abstract published in *Advance ACS Abstracts,* August 15, 1997.

S0024-9297(97)00210-6 CCC: $14.00

determined from data for the mixture.

Both the classic and compressible versions of FH theory contain the combinatorial entropy for packing the chains of the different blend species, but the compressible approach introduces the additional translation contribution to the entropy which may also be interpreted as describing the distribution of excess free volume in the blend. The Flory−Orwoll−Vrij equation-of-state theories[11] retain the same spirit as the compressible FH approach, except for the use of a more realistic description of this translational entropy, but only at the expense of introducing additional adjustable parameters. The compressible FH theory begins with a similar free energy expression as used in Sanchez−Lacombe (SL) theory.[12] However, the latter FH formulation, when applied to a pure melt, employs only two microscopic parameters, the self-interaction energy ϵ_{ii} and the cell volume v_{cell}, whereas SL theory translates these two microscopic parameters into three physically reasonable macroscopic phenomenological thermodynamic parameters, the reduced pressure P^*, temperature T^*, and specific volume v^*, which appear to be necessary for SL theory to provide an accurate description of melt equations-of-state data. Both FH and SL approaches require some additional combining rules in their extensions to binary blends.

There is a broad literature concerning experimental studies of binary random copolymer blends. For example, a series of papers by Paul and co-workers determine[13,14] the interaction parameters by fitting the Sanchez−Lacombe theory to *PVT* data for the pure melts and to experimental phase boundaries. A wide variety of miscibility patterns is then analyzed in terms of these parameters. As emphasized[14] by Paul and coworkers, the empirical interaction energies only have utility for predicting phase behavior when employed within the same theoretical approach from which they are deduced. This body of work serves to exhibit the expected superiority of the Sanchez−Lacombe approach[12] over standard incompressible FH theory[1,4] for modeling the phase diagrams, but experimental miscibility patterns pose several challenges for theory.

For example, experimental phase diagrams[15] for blends of two random copolymers, containing the same monomer units but differing in composition, display isothermal miscibility domains that sometimes lie between two parallel straight lines as predicted by FH-like theories. However, more often the phase diagrams yield[15] boundaries with substantial convexities relative to the diagonal, especially for blends of branched copolymers. Chai *et al.*[15] explain the convex phase boundaries as arising from the dependence of the effective interaction parameter χ_{eff} on the monomer sequence distributions. The effective interaction parameter for A_xB_{1-x}/A_yB_{1-y} polyolefin blends has been found[16−18] to depend not only on the compositional difference $\delta = |x - y|$, as predicted by incompressible random copolymer FH theory,[1,4] but also on the averaged composition $s = (x + y)/2$. Different compatibilities of A_xB_{1-x}/A and A_xB_{1-x}/B random copolymer/homopolymer systems are reported by Russell et al.[19] and Winey et al.,[20] a feature that departs for x = 0.5 from the predictions of random copolymer FH theory.[1]

The compressible extension of random copolymer FH theory is applied here to study the influence of compressibility on the miscibility of A-*co*-B random copolymer mixtures with their respective homopolymers A or B and of blends containing two A-*co*-B random copolymers with different compositions. Because FH type theory contains purely energetic, composition independent interaction parameters, even the compressible extension cannot describe homopolymer blends with a lower critical solution temperature (LCST). Hence, we also extend the FH type treatment by including a simple model of the leading contribution to the noncombinatorial entropy as determined from the LCT for homopolymer blends. This entropic term contains no additional adjustable parameters and provides an additional mechanism for LCST behavior than the one generally invoked.[12,21] This simple homopolymer blend model for the noncombinatorial entropy employs only an approximation to the leading nonrandom mixing terms and ignores all other contributions, such as those arising from a monomer sequence dependence, which will be included in a future work[9] based on the full LCT. Sanchez−Lacombe theory[12] and the Flory−Orwoll−Vrij equation-of-state theory,[11] on the other hand, can predict a LCST phase diagram, in part, because of the use of three macroscopic parameter P^*, T^*, and v^* and specific combining rules. However, these approaches lack a simple microscopic interpretation which, we believe, is necessary for passing on to the more detailed molecular level of description required for the control and design of polymer systems with desired specific properties.

Section II reviews the basic background for generalizing FH theory to compressible binary random copolymer mixtures and outlines the simple model for the noncombinatorial entropy of these systems. Sections III and IV describe several illustrative computations of miscibility gaps, pressure dependence, critical temperature variations, etc. for A_xB_{1-x}/A,B and for A_xB_{1-x}/A_yB_{1-y} blends, respectively.

II. Compressible FH Type Theory for Random Copolymer Systems

A. Free Energy for A_xB_{1-x}/A and A_xB_{1-x}/B Systems. Blends of an A_xB_{1-x} random copolymer and homopolymer A or B are the simplest examples of binary systems containing random copolymers. The Helmholtz free energy F per lattice side is given by

$$\frac{F}{N_1 k_B T} = \phi_v \ln \phi_v + \frac{\phi_1}{M_1} \ln \phi_1 + \frac{\phi_2}{M_2} \ln \phi_2 - \frac{z}{2k_B T}\phi_1^2[\epsilon_{AA}x^2 + \epsilon_{BB}(1-x)^2 + 2\epsilon_{AB}x(1-x)] - \frac{z}{2k_B T}\phi_2^2\epsilon_{CC} - \frac{z}{k_B T}\phi_1\phi_2[\epsilon_{AC}x + \epsilon_{BC}(1-x)] \quad (2.1)$$

where the subscripts 1 and 2 refer to the random copolymer A_xB_{1-x} and the homopolymer C = A, B, respectively, ϕ_1 and ϕ_2 are the actual volume fractions normalized as $\phi_1 + \phi_2 = 1 - \phi_v$ (with ϕ_v denoting the volume fraction of excess free volume), M_1 and M_2 designate the polymerization indices, $\epsilon_{\alpha\beta}$ are the nearest neighbor attractive van der Waals energies, and z is the lattice coordination number. Terms linear in ϕ_1 and ϕ_2 are omitted in eq 2.1 as being thermodynamically irrelevant, i.e., as not affecting the equation of state or the phase stability limit. Since attractive energies $\epsilon_{\alpha\beta}$ are taken in our convention as positive quantities, the energetic terms of eq 2.1 appear with minus signs. The free volume fraction ϕ_v is determined from the equation of state as a function of pressure P and temperature T for a given blend composition $\Phi_1 = \phi_1/(1 - \phi_v) = 1 - \Phi_2$

and for the cell volume v_{cell} associated with a single lattice site.

Introducing the compact notation

$$\chi_{11} \equiv -\frac{z}{2k_BT}[\epsilon_{AA}x^2 + \epsilon_{BB}(1-x)^2 + 2\epsilon_{AB}x(1-x)] \tag{2.2a}$$

$$\chi_{22} \equiv -\frac{z}{2k_BT}\epsilon_{CC} \tag{2.2b}$$

and

$$\chi_{12} \equiv -\frac{z}{2k_BT}[\epsilon_{AC}x + \epsilon_{BC}(1-x)] \tag{2.2c}$$

converts eq 2.1 into the well-known universal form for all compressible binary blends

$$\frac{F}{N_l k_B T} = \phi_v \ln \phi_v + \frac{\phi_1}{M_1}\ln \phi_1 + \frac{\phi_2}{M_2}\ln \phi_2 + \phi_1{}^2\chi_{11} + \phi_2{}^2\chi_{22} + 2\phi_1\phi_2\chi_{12} \tag{2.3}$$

The two interaction parameters χ_{11} and χ_{12} depend on the copolymer composition x. Applying the incompressible limit $\phi_v \to 0$ ($\phi_1 + \phi_2 = 1$) to eq 2.3 recovers the FH type free energy expression of Kambour *et al.*[1] and ten Brinke *et al.*[4]

$$\frac{F}{N_l k_B T} = \frac{\phi_1}{M_1}\ln \phi_1 + \frac{\phi_2}{M_2}\ln \phi_2 + \phi_1\phi_2\chi \tag{2.4}$$

where the interaction parameter $\chi \equiv -\chi_{11} - \chi_{22} + 2\chi_{12}$ is related to the Flory interaction parameter χ_{AB}

$$\chi_{AB} \equiv \frac{z}{2k_BT}[\epsilon_{AA} + \epsilon_{BB} - 2\epsilon_{AB}] \tag{2.5}$$

for binary A/B blends by

$$\chi = \begin{cases} (1-x)^2\chi_{AB}, & \text{if C = A} \\ x^2\chi_{AB}, & \text{if C = B} \end{cases} \tag{2.5a}$$

Both cases become identical for $x = 1/2$, a special symmetry of the FH type approach.

Lifting the incompressibility assumption breaks the special symmetry for $x = 1/2$. To make this feature even more apparent, eq 2.1 is reexpressed as

$$\frac{F(C=A) - F(C=B)}{N_l k_B T} = \phi_1\phi_2\chi_{AB}(1-2x) + \frac{z}{2k_BT}\phi_1\phi_v(\epsilon_{AA} - \epsilon_{BB}) \tag{2.6}$$

Equation 2.6 clearly demonstrates that the $x = 1/2$ symmetry is broken for the compressible A_xB_{1-x}/A and A_xB_{1-x}/B systems when the self-interaction energies ϵ_{AA} and ϵ_{BB} differ, a situtation generally occurring because of disparate reduced temperatures T^*(A) and T^*(B) for the pure melts A and B. Since FH type theories treat the monomers as totally devoid of structure, the occurrence of equal interaction energies ϵ_{AA} and ϵ_{BB} probably ensues only with the complete identity of monomers A and B because $\epsilon_{AA} \neq \epsilon_{BB}$ emerges even when B is the perdeuterated analog of A.

B. Free Energy for A_xB_{1-x}/A_yB_{1-y} Blends. The simplest mean field Helmholtz free energy for compressible blends of two random copolymers A_xB_{1-x} and A_yB_{1-y} depends on both composition variables x and y as

$$\frac{F}{N_l k_B T} = \phi_v \ln \phi_v + \frac{\phi_1}{M_1}\ln \phi_1 + \frac{\phi_2}{M_2}\ln \phi_2 - \frac{z}{2k_BT}\phi_1{}^2[\epsilon_{AA}x^2 + \epsilon_{BB}(1-x)^2 + 2\epsilon_{AB}x(1-x)] - \frac{z}{2k_BT}\phi_2{}^2[\epsilon_{AA}y^2 + \epsilon_{BB}(1-y)^2 + 2\epsilon_{AB}y(1-y)] - \frac{z}{2k_BT}\phi_1\phi_2[\epsilon_{AA}xy + \epsilon_{BB}(1-x)(1-y) + \epsilon_{AB}\{x(1-y) + y(1-x)\}] \tag{2.7}$$

where the subscripts 1 and 2 label the copolymers A_xB_{1-x} and A_yB_{1-y}, respectively. The noncombinatorial contributions to the free energy F in eq 2.7 (as in eq 2.1) can be generated easily from the lattice cluster theory[9,22] (where they represent the zeroth order approximation) by considering only the leading first-order energy diagram with a single interaction line connecting two uncorrelated (nonbonded) monomers which are chosen from the all monomers in the system.

The general form (eq 2.3) still applies to the free energy F in eq 2.7, but the macroscopic interaction parameters χ_{ij} become

$$\chi_{11} \equiv -\frac{z}{2k_BT}[\epsilon_{AA}x^2 + \epsilon_{BB}(1-x)^2 + 2\epsilon_{AB}x(1-x)] \tag{2.8a}$$

$$\chi_{22} \equiv -\frac{z}{2k_BT}[\epsilon_{AA}y^2 + \epsilon_{BB}(1-y)^2 + 2\epsilon_{AB}y(1-y)] \tag{2.8b}$$

and

$$\chi_{12} \equiv -\frac{z}{2k_BT}[\epsilon_{AA}xy + \epsilon_{BB}(1-x)(1-y) + \epsilon_{AB}\{x(1-y) + y(1-x)\}] \tag{2.8c}$$

and are now more complicated functions of composition and interaction energies than those describing the A_xB_{1-x}/C = A,B systems. Setting $\phi_v = 0$ (i.e., $\phi_1 + \phi_2 = 1$) transforms eq 2.7 into the well-known incompressible system ($P \to \infty$) FH type expression[4]

$$\frac{F}{N_l k_B T} = \frac{\phi_1}{M_1}\ln \phi_1 + \frac{\phi_2}{M_2}\ln \phi_2 + \phi_1\phi_2(x-y)^2\chi_{AB} \tag{2.9}$$

with χ_{AB} given by eq 2.5.

C. Stability Limits for A_xB_{1-x}/C = A,B and A_xB_{1-x}/A_yB_{1-y} Blends. A binary blend at constant pressure P is stable (or metastable)[23] if the first derivative of the chemical potential μ_1 of polymer species 1 with respect of its volume fraction Φ_1 is positive

$$\left.\frac{\partial \mu_1}{\partial \Phi_1}\right|_{P,T} > 0 \tag{2.10}$$

Setting the left hand side of the inequality (eq 2.10) to zero produces the stability limit (called the "spinodal") at constant P as determined by

$$\left.\frac{\partial \mu_1}{\partial \Phi_1}\right|_{P,T} = 0 \tag{2.11}$$

Both the pressure P and the chemical potential μ_1 are obtained from the Helmholtz free energy F of eq 2.3 as

$$P = -\left.\frac{\partial F}{\partial V}\right|_{T,n_1,n_2} = -\frac{1-\phi_v}{v_{\rm cell}\, N_1}\left.\frac{\partial F}{\partial \phi_v}\right|_{T,n_1,n_2} \qquad (2.12)$$

and

$$\mu_1 = \left.\frac{\partial F}{\partial n_1}\right|_{V,T,n_2} \qquad (2.13)$$

where n_1 and n_2 designate the numbers of polymer chains of blend species 1 and 2, respectively, $V = N_1 v_{\rm cell}$ denotes the total volume of the system, and the cell volume $v_{\rm cell}$ is assumed, for simplicity, to be a temperature-independent quantity. The equation of state, derived from eq 2.12, enables us to evaluate the derivative $\partial\phi_v/\partial\Phi_1$ at constant P. The spinodal condition (eq 2.11) is thereby converted to

$$\left[\frac{1}{\phi_v} + \frac{\Phi_1}{M_1(1-\phi_v)} + \frac{\Phi_2}{M_2(1-\phi_v)} + 2\chi_{11}\Phi_1^{\,2} + 2\chi_{22}\Phi_2^{\,2} + 4\chi_{12}\Phi_1\Phi_2\right]\left[\frac{1}{M_1\Phi_1} + 2(1-\phi_v)(\chi_{11}-\chi_{22})\right] - \left[\frac{1}{\phi_v} + \frac{1}{M_1(1-\phi_v)} + 2\chi_{11}\Phi_1 + 2\chi_{12}\Phi_2\right]\left[\frac{1}{M_1} - \frac{1}{M_2} + 2(1-\phi_v)\{\chi_{11}\Phi_1 - \chi_{22}\Phi_2 + \chi_{12}(1-2\Phi_1)\}\right] = 0 \qquad (2.14)$$

with $\chi_{ij}(T)$ defined by eqs 2.2a−c and 2.8a−c for A_xB_{1-x}/C = A,B and A_xB_{1-x}/A_yB_{1-y} blends, respectively, and with $\Phi_2 = 1 - \Phi_1$. The spinodal equation (eq 2.14) does not admit an analytical solution for $T = T(\Phi_1)$ because the free volume fraction ϕ_v must be determined from the equation of state for given P, T, M_i, Φ_1, etc.

Equation 2.14 simplifies in the incompressible limit ($\phi_v \to 0$, $1/\phi_v \to \infty$) to the standard RPA form,

$$\frac{1}{M_1\Phi_1} + \frac{1}{M_2\Phi_2} - 2\chi = 0 \quad (P \to \infty) \qquad (2.15)$$

where $\chi \equiv -\chi_{11} - \chi_{22} + 2\chi_{12}$. The expression (eq 2.15) can be also recovered from the incompressible limit of the constant volume spinodal condition. The constant volume stability limit for a binary blend is evaluated from the stability condition

$$\left.\frac{\partial^2 F}{\partial \phi_1^{\,2}}\right|_{V,\phi_2}\left.\frac{\partial^2 F}{\partial \phi_2^{\,2}}\right|_{V,\phi_1} - \left[\left.\frac{\partial^2 F}{\partial\phi_1\partial\phi_2}\right|_V\right]^2 = 0 \qquad (2.16)$$

as

$$\left[\frac{1}{M_1\phi_1} + \frac{1}{M_2\phi_2} - 2\chi\right] + \phi_v\left[\frac{1}{M_1M_2\phi_1\phi_2} + \frac{2\chi_{11}}{M_2\phi_2} + \frac{2\chi_{22}}{M_1\phi_1} + 4(\chi_{11}\chi_{22} - \chi_{12}^{\,2})\right] = 0 \qquad (2.17)$$

Equation 2.17, indeed, reduces (as it must) to eq 2.15 when $\phi_v = 0$. The term $4(\chi_{11}\chi_{22} - \chi_{12}^{\,2})$ in eq 2.17 is a measure of deviations for the heterocontact energy ϵ_{AB} from the Berthelot combining rule[24] value and vanishes identically when $\epsilon_{AB} = (\epsilon_{AA}\epsilon_{BB})^{1/2}$. The term $2\chi_{22}/(M_1\phi_1)$ in eq 2.17 generally imparts a difference between the two $A_{1/2}B_{1/2}$/C = A,B systems. However, when the blends are treated as incompressible this term no longer influences the stability condition in eq 2.17. Hence, eqs 2.15 and 2.17 indicate that incompressible $A_{x=1/2}B_{1-x}$/A and $A_{x=1/2}B_{1-x}$/B blends would both produce identical spinodals because the respective effective interaction parameters $\chi = (1-x)^2\chi_{AB}$ and $\chi = x^2\chi_{AB}$ become the same for $x = {}^1/_2$. Since the constant volume condition implies the constancy of ϕ_v, eq 2.17 can be solved analytically in the form $T = T(\Phi_1, M_1, M_2, \ldots)$.

D. Modification of FH Type Theories To Describe LCST Random Copolymer Systems. Both incompressible and compressible versions of FH type theories predict complete miscibility at all temperatures for systems exhibiting a negative energy $\epsilon = \epsilon_{11} + \epsilon_{22} - 2\epsilon_{12}$, i.e., for systems that usually exhibit a LCST phase diagram. In order to generate LCST phase diagrams from these theories with composition independent interaction parameters χ_{ij} (see eqs 2.2a−c and 2.8a−c), the $\{\chi_{ij}\}$ must also contain entropic (i.e., temperature independent) contributions $\chi_{ij}^{\rm ent}$, and the combination $\chi^{\rm ent} \equiv \chi_{11}^{\rm ent} + \chi_{22}^{\rm ent} - 2\chi_{12}^{\rm ent}$ must be positive and sufficiently large to overcome the attractive enthalpic portion. Because the fitting of three new parameters $\chi_{ij}^{\rm ent}$ is highly undesirable, we use the homopolymer LCT to provide a model for specifying these $\chi_{ij}^{\rm ent}$ without introducing adjustable parameters. This model is introduced here in advance of a more accurate, but more tedious, LCT treatment,[9] which includes influences of nonrandom mixing, sequence dependence, etc.

The LCT yields an estimation of the entropic contribution to the A/B binary blend effective interaction parameter χ_{AB} that favorably compares[25,26] with experiments for the well-studied PS/PVME blend. In the athermal limit of infinite molecular weights ($M_1, M_2 \to \infty$) and pressures ($P \to \infty$), the LCT expression for $\chi_{AB}^{\rm ent}$ simplifies to the form[27]

$$\chi_{AB}^{\rm ent} = \frac{1}{z^2}\left[\frac{N_2^{(1)}}{M_1} - \frac{N_2^{(2)}}{M_2}\right]^2 \qquad (2.18)$$

where the geometrical coefficients $N_2^{(i)}$ designate the numbers of ways for selecting two consecutive bonds in a single chain of polymer species i and where z denotes the lattice coordination number. The ratios $r_i \equiv N_2^{(i)}/M_i$ may be expressed[28] more conveniently in terms of the fractions of tri- and tetrafunctional units within the LCT united atom, structured monomer model for the chains and may therefore easily be evaluated.

The entropically modified interaction parameters χ'_{ij} are chosen for an A_xB_{1-x}/C (C = A,B) blend by analogy with the forms in eq 2.2 as

$$\chi'_{11} = \chi_{11} + x^2\chi_{AA}^{\rm ent} + (1-x)^2\chi_{BB}^{\rm ent} + 2x(1-x)\chi_{AB}^{\rm ent} \qquad (2.19a)$$

$$\chi'_{22} = \chi_{22} + \chi_{CC}^{\rm ent} \qquad (2.19b)$$

and

$$\chi'_{12} = \chi_{12} + x\chi_{AC}^{\rm ent} + (1-x)\chi_{BC}^{\rm ent} \qquad (2.19c)$$

where and $\chi_{ij} \propto 1/T$ are the original interaction parameters of eq 2.2a−c and $\chi_{\alpha\beta}^{\rm ent} \equiv -(1/z^2)(N_2^{(\alpha)}/M_\alpha)(N_2^{(\beta)}/M_\beta)$ (α,β = A,B). The resulting FH type theory is then consistent with the limiting behavior of eq 2.18. In addition, eq 2.19 is designed to pass smoothly from the proper $x = 0$ to $x = 1$ limits, i.e., from the description of a B/C to an A/C homopolymer blend. The use of the χ'_{ij}

from eq 2.19 enables the theory to explain the fact that some blends separate upon heating without employing additional adjustable parameters. The appropriate generalization of eq 2.8 to provide the χ'_{ij} for blends of two random copolymers A_xB_{1-x} and A_yB_{1-y} then follows as

$$\chi'_{11} = \chi_{11} + x^2\chi_{AA}^{ent} + (1-x)^2\chi_{BB}^{ent} + 2x(1-x)\chi_{AB}^{ent} \quad (2.20a)$$

$$\chi'_{22} = \chi_{22} + y^2\chi_{AA}^{ent} + (1-y)^2\chi_{BB}^{ent} + 2y(1-y)\chi_{AB}^{ent} \quad (2.20b)$$

and

$$\chi'_{12} = \chi_{12} + x\,y\,\chi_{AA}^{ent} + (1-x)(1-y)\chi_{BB}^{ent} + [x(1-y) + y(1-x)]\chi_{AB}^{ent} \quad (2.20c)$$

where the original unmodified χ_{ij} are defined by eq 2.8a−c and where the same notation $\chi_{\alpha\beta}^{ent} \equiv -(1/z^2)(N_2^{(\alpha)}/M_\alpha)(N_2^{(\beta)}/M_\beta)$ is employed. We note that the full LCT would produce[9] a more complex expressions than eqs 2.19 and 2.20 from the inclusion of local correlations, sequence dependence, contributions of order $\epsilon_{\alpha\beta}^2$, etc.

III. Computations of Phase Diagrams for $A_xB_{1-x}/C = A,B$ Blends

The phase behavior of $A_xB_{1-x}/C = A,B$ mixtures is illustrated by considering PS_xPMMA_{1-x}/PS (or PMMA) and PS_xPVME_{1-x}/PS (or PVME) blends which exhibit, respectively, upper and lower critical solution temperatures. This choice of systems ensures evidencing a wide range of possible miscibility patterns. All phase diagrams (spinodals), except for those in the incompressible limit, are computed at a constant pressure of 1 atm, and both components in each blend are assumed, for simplicity, to have the same polymerization indices $M_1 = M_2 = M$. (The subscript 1 always designates the random copolymer, whereas component 2 is the pure homopolymer.) The lattice coordination number z is six and merely enters into the equations of section II as a scaling factor between the macroscopic interaction parameters χ_{ij} and the microscopic van der Waals nearest neighbor energies ϵ_{ij}. The only adjustable parameters in eq 2.14 are, therefore, the van der Waals energies $\{\epsilon_{ij}\}$ and the unit cell volume v_{cell}. The former are fit to available experimental data for the pure melts of species A and B, respectively, and for their blend A/B, while the latter is determined, as explained below, by applying a standard combining rule[29] relating the blend cell volume to those $v_{cell}^{(i)}$ for the pure blend components. Since the free volume fraction $\phi_v = \phi_v(P,T,M,\{\epsilon_{ij}\},\Phi_1,x,v_{cell})$ is computed from the equation of state, the solution $T = T(\Phi_1)$ of eq 2.14 is available only in numerical form.

The standard philosophy of mixture theory for determining the self interaction energies ϵ_{11} and ϵ_{22} involves fitting the respective equations of state for the pure melt to *PVT* data over a wide range of pressures and temperatures. The required melt free energy is generated simply from eq 2.1 by setting $\phi_1 = 0$. A two-parameter least-squares fit produces the energy ϵ_{ii} and the cell volume $v_{cell}^{(i)}$ for each of the two blend species. The resultant two-parameter equation of state poorly reproduces melt experimental *PVT* data over a wide pressure range when ϵ_{ii} and $v_{cell}^{(i)}$ are taken as pressure independent. (The LCT, on the other hand, has no additional adjustable parameters and fares very well![25]) Therefore, our fits of ϵ_{ii} and $v_{cell}^{(i)}$ are limited to data for $P = 1$ atm, when available. The prime focus here lies in describing general features of phase diagrams for random copolymer systems at ambient pressures, so a very precise determination of the parameters is not required for illustrating the general behavior.

A. PS_xPMMA_{1-x}/PS and PS_xPMMA_{1-x}/PMMA Systems. A two-parameter fit to the $P = 1$ atm data for PS yields $\epsilon_{S-S} = 0.6234k_BT_o$ ($T_o = 415.5$ K) and $v_{cell}^{(S)} = 158.79$ A^3. This $\epsilon_{S-S} = 0.6234k_BT_o$ coincides with the value obtained by us from fitting[25] the full LCT equation of state to PVT data at pressures ranging from 1 to 1000 atm. The cell volume $v_{cell}^{(S)}$ is larger by a factor of 9 than the corresponding quantity in the LCT fit, a difference resulting because one styrene monomer extends over $s = 9$ lattice sites in the LCT description,[25,27] while it occupies $s = 1$ lattice site in the FH approach. Hence, the factor of 9 exhibits the internal consistency between the two fits. This internal consistency for ϵ_{S-S} is used below to determine ϵ_{ii} and $v_{cell}^{(i)}$ for the PMMA melt where *PVT* data are not available at $P = 1$ atm or even slightly elevated pressures. Consequently, the self-interaction energy $\epsilon_{MMA-MMA} = 0.593k_BT_o$ given above is taken from our LCT fits[25] to the 1 atm SANS data for the PS-*b*-PMMA diblock copolymer system, while the cell volume $v_{cell}^{(MMA)}$ is assumed to be 7-fold larger than the value $v_{cell}^{(LCT)} = 19.06$ A^3 obtained from that LCT analysis as described in ref. 25 because the occupancy indices are $s = 7$ and $s = 1$ for a methyl methacrylate monomer in the LCT and FH compressible theory, respectively. The difference in the cell volumes $v_{cell}^{(MMA)}$ and $v_{cell}^{(LCT)}$ reflects the disparity in monomer sizes.

The cell volume v_{cell} for the PS_xPMMA_{1-x}/PS system is evaluated from the standard combining rule[29] as

$$v_{cell} = \Phi_1^2 v_{cell}^{(1)} + \Phi_2^2 v_{cell}^{(2)} + (1/4)\Phi_1\Phi_2[(v_{cell}^{(1)})^{1/3} + (v_{cell}^{(2)})^{1/3}]^3 \quad (3.1)$$

where $v_{cell}^{(1)}$ is given for the random copolymer by

$$v_{cell}^{(1)} = v_{cell}^{(S)}\,x + v_{cell}^{(MMA)}(1-x) \quad (3.2)$$

and for the homopolymer simply by

$$v_{cell}^{(2)} = v_{cell}^{(S)}$$

Equation 3.1 applies to a PS_xPMMA_{1-x}/PMMA mixture with the obvious modification of taking $v_{cell}^{(2)} = v_{cell}^{(MMA)}$. The remaining heterocontact interaction energy $\epsilon_{S-MMA} = 0.5984k_BT_o$ is determined from a rough fit to the cloud-point data of Callaghan and Paul[30] for binary PS/PMMA blends. The fit is based on the simplified version of eqs 2.2a−c and 2.14 which for $x = 1$ describes a PS/PMMA homopolymer blend. The knowledge of these four parameters ($\{\epsilon_{ij}\}$ and v_{cell}) allows us to compute the spinodal curves for PS_xPMMA_{1-x}/PS and PS_xPMMA_{1-x}/PMMA mixtures by using eq 2.14 with the interaction parameters χ_{ij} given by eq 2.2a−c and with the free volume fraction ϕ_v determined from the equation of state in eq 2.12.

We begin the analysis of the miscibility for PS_xPMMA_{1-x}/PS and PS_xPMMA_{1-x}/PMMA blends by considering systems with symmetric random copolymers, i.e. characterized by $x = 1/2$. While incompressible FH

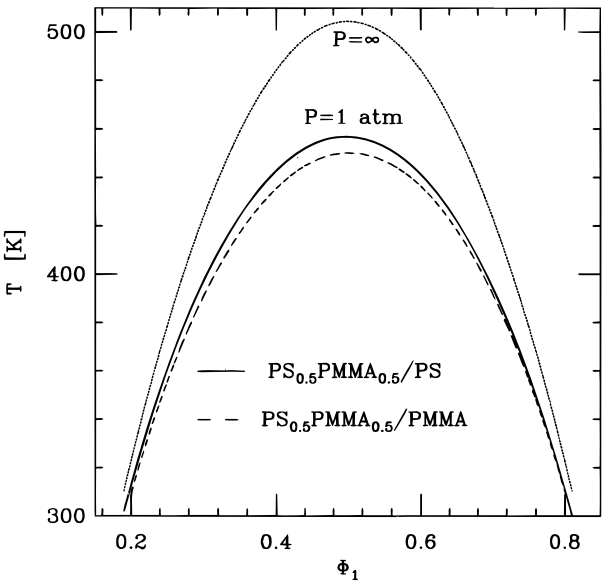

Figure 1. Spinodal curves for $PS_{0.5}PMMA_{0.5}$/PS and $PS_{0.5}$-$PMMA_{0.5}$/PMMA mixtures at $P = 1$ atm and at $P = \infty$. The infinite pressure phase diagram corresponds to the classic prediction of incompressible FH theory. The polymerization indices for the two polymer blend species are assumed to be equal $M_1 = M_2 = 200$. Subscript 1 labels the random copolymer, while subscript 2 refers to the homopolymer. The same M_1 and M_2 apply to Figures 2 and 3.

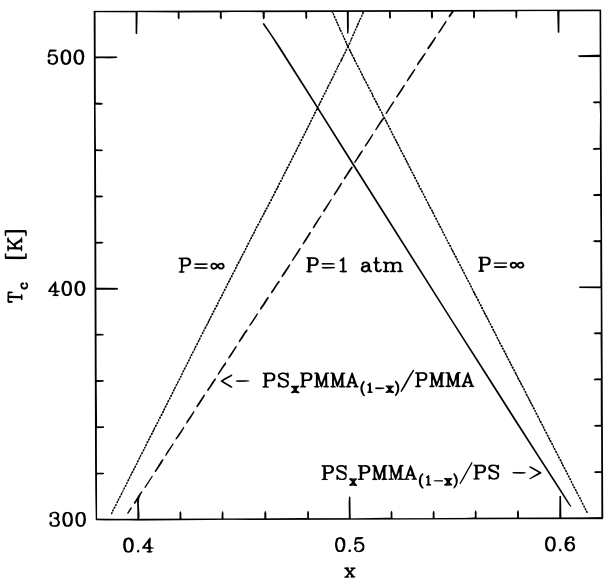

Figure 2. Variations of the critical temperature T_c with composition x for PS_xPMMA_{1-x}/PS and PS_xPMMA_{1-x}/PMMA mixtures (at $P = 1$ atm and at $P = \infty$).

theory does not distinguish between $PS_{1/2}PMMA_{1/2}$/PS and $PS_{1/2}PMMA_{1/2}$/PMMA mixtures (see eqs 2.5a and 2.15) with corresponding polymerization indices, the compressible extension of the FH mean field approximation predicts that the symmetric random copolymer $PS_{1/2}PMMA_{1/2}$ mixes slightly better with PMMA than with PS. This prediction is illustrated in Figure 1, which also presents the phase diagram generated from incompressible FH theory. The latter phase diagram is common for both blends and corresponds to the infinite pressure limit of the compressible treatments. Figure 1 exhibits some differences in the miscibility of the symmetric random copolymer with the two homopolymers but not the rather huge experimentally observed[20] disparity in the miscibilities of $PS_{1/2}PMMA_{1/2}$/PS and $PS_{1/2}PMMA_{1/2}$/PMMA blends. Figure 1 also demonstrates the significant influence of pressure on the miscibility of random copolymer systems, an influence that should not be ignored in quantitative studies. An increase in pressure renders both systems less miscible, a behavior quite typical in LCT computations[28] for upper critical solution temperature binary homopolymer systems.

As in traditional FH random copolymer treatments, the relative miscibilities of PS_xPMMA_{1-x}/PS and PS_x-$PMMA_{1-x}$/PMMA blends are predicted to depend on the percentage of PS and PMMA in the random copolymer, i.e. on its composition x. When x grows, the critical temperature T_c for the PS_xPMMA_{1-x}/PS blend diminishes (since its miscibility improves). The critical temperature T_c for the PS_xPMMA_{1-x}/PMMA mixture, in contrast, increases with x, indicating a worsened miscibility. This behavior, depicted in Figure 2, is common to both incompressible and compressible versions of FH type theories and can be inferred easily from the observation that similar polymer species mix better.

Figure 2 also demonstrates that the critical temperatures for PS_xPMMA_{1-x}/PS and PS_xPMMA_{1-x}/PMMA mixtures become identical for $x^* = 0.5025$ in the compressible FH type theory and for $x = 0.5$ in standard FH theory. When $x < x^*$, the PS_xPMMA_{1-x}/PMMA blend is more miscible than PS_xPMMA_{1-x}/PS, but when $x > x^*$, the trend reverses. These predictions are in accord in a limited sense with the experimental data of Russell and co-workers[19] who report drastic changes in the miscibility of PS_xPMMA_{1-x} with PS or PMMA depending on the random copolymer composition. For instance, PS_xPMMA_{1-x} with 90% of PS does not mix with PMMA but mixes with pure PS up to a 15% weight fraction, while a decrease of the PS content in PS-*co*-PMMA from 90% to 30% leads to the opposite miscibility patterns.[19] In spite of the fact that both incompressible and compressible versions of FH theories predict similar values of x^*, the two theoretical approaches yield significantly differing critical temperatures over a wide range of compositions x.

An alternative illustration for the influence of compressibility on random copolymer blend miscibilities is provided by Figure 3, which presents the critical temperatures for PS_xPMMA_{1-x}/PS and PS_xPMMA_{1-x}/PMMA, respectively, versus $(1 - x)^2$ and x^2. Classic FH theory (see eq 2.5a) predicts one straight line of the form $T_c = \alpha_T(1 - x)^2$ or $T_c = \alpha_T x^2$ [with slope $\alpha_T = (1/4)Mz\epsilon/k_B$] for both of these two systems, while the compressible extension yields distinct curves in Figure 3. For given x, $T_c^{\infty} \equiv T_c^{(P=\infty)}$ is greater than T_c, and larger differences $\delta_T \equiv T_c^{(P=\infty)} - T_c$ emerge when the random copolymer PS_xPMMA_{1-x} is blended with the minority homopolymer, i.e., for the less miscible system.

A summary of the phase diagrams for many systems of the same species but different molecular weights is provided by presenting the critical polymerization index M_c for phase separation that occurs at a given temperature T_c in a binary system with equal polymerization indices $M_1 = M_2 = M$. Figure 4 depicts this critical polymerization index for PS_xPMMA_{1-x}/PS and PS_x-$PMMA_{1-x}$/PMMA as a function of $(1 - x)^{-2}$ and x^{-2}, respectively. Again, classic FH random copolymer theory yields only a single line $M_c = \alpha_M(1 - x)^{-2}$ or $M_c = \alpha_M x^{-2}$ [with slope $\alpha_M = 4/(z\epsilon)$] for these two blends. In contrast, we find that $M_c^{(\infty)} < M_c$, and larger deviations $\delta_M \equiv M_c - M_c^{(\infty)}$ appear for PS_xPPMA_{1-x}/PS with high x and for PS_xPMMA_{1-x}/PMMA with low x, i.e., for the more miscible systems.

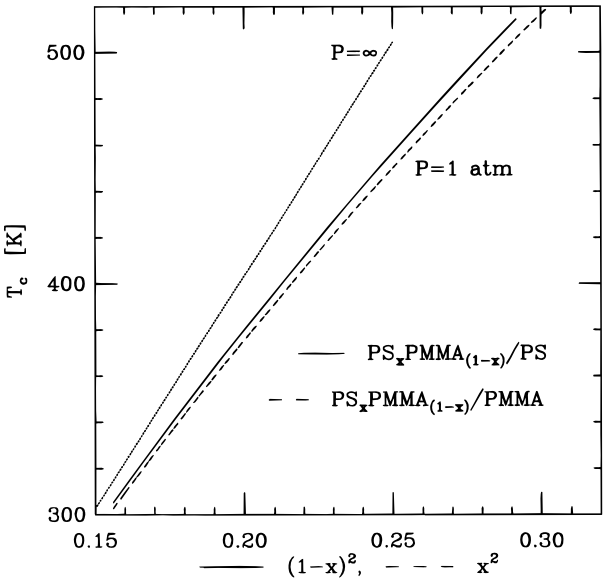

Figure 3. Critical temperature T_c of PS_xPMMA_{1-x}/PS and PS_x-$PMMA_{1-x}$/PMMA blends as a function of $(1 - x)^2$ and x^2, respectively. Only classic FH theory predicts a linear behavior of T_c with $(1 - x)^2$ or with x^2.

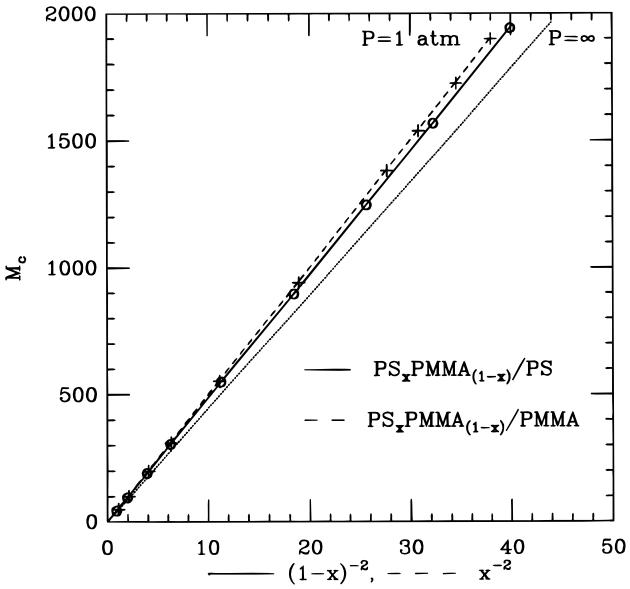

Figure 4. Critical polymerization index M_c for symmetric PS_x-$PMMA_{1-x}$/PS and PS_xPMMA_{1-x}/PMMA blends at $T = 450$ K as a function of $(1 - x)^{-2}$ and x^{-2}, respectively. Both incompressible and compressible versions of FH theory produce a linear behavior of M_c with $(1 - x)^{-2}$ or x^{-2}.

B. UCST Systems with More Asymmetric Self-Interactions. The attractive van der Waals energies ϵ_{ij} in FH type theories are the only parameters reflecting the chemistry of the system because monomer molecular structure is completely ignored. Thus, it is worth considering how the trends in Figures 1−4 compare with those generated by using a different set $\{\epsilon_{ij}\}$, characterizing other UCST A_xB_{1-x}/C = A,B blends with more disparate A and B self-interaction energies. We retain $\epsilon_{11} = 0.62k_BT_o$, but admit a much less attractive ϵ_{22} by assuming $\epsilon_{22} = 0.5k_BT_o$. The heterocontact interaction energy ϵ_{12} is taken as the geometrical mean $\epsilon_{12} = (\epsilon_{11}\epsilon_{22})^{1/2}$. The use of the Berthelot combining rule[24] guarantees a positive exchange energy $\epsilon = \epsilon_{11} + \epsilon_{22} - 2\epsilon_{12}$ and the existence of an UCST phase diagram. The choice of the cell volume v_{cell} is fairly irrelevant because the computed phase diagrams at $P = 1$ atm are found to be very insensitive even to large changes of v_{cell}. Hence, we employ the same v_{cell} as applied to describe the PS_xPMMA_{1-x}/PS and PS_xPMMA_{1-x}/PMMA mixtures.

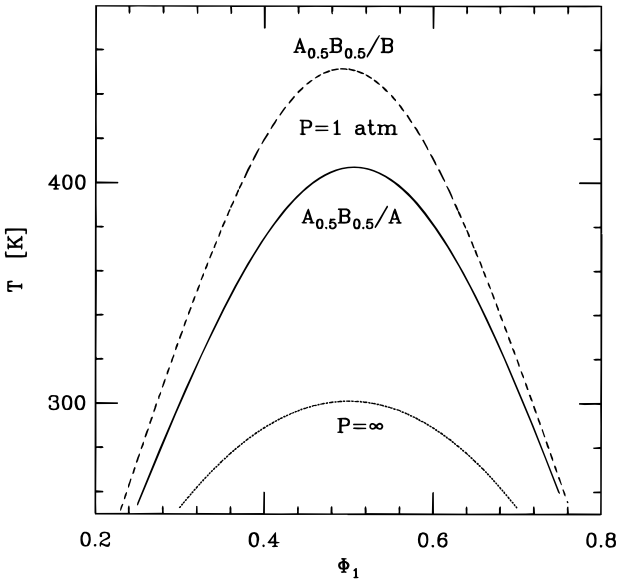

Figure 5. Spinodal curves for model UCST $A_{0.5}B_{0.5}$/A and $A_{0.5}B_{0.5}$/B mixtures at $P = 1$ atm and $P = \infty$. The infinite pressure spinodal corresponds to the prediction of classic FH theory. The polymerization indices are chosen as $M_1 = M_2 = 300$ and are also used in Figures 6−8.

The presence of more disparate self-interaction energies introduces profound differences into the phase diagrams of $A_{0.5}B_{0.5}$/A and $A_{0.5}B_{0.5}$/B blends. Figure 5 shows that the critical temperatures for these two symmetrical random copolymer mixtures differ by almost 50 K, while the critical compositions are practically the same, deviating slightly from the symmetric value of $\Phi_1 = 0.5$. As mentioned earlier, standard random copolymer FH theory does not distinguish between the $A_{0.5}B_{0.5}$/A and $A_{0.5}B_{0.5}$/B systems (with corresponding polymerization indices) and produces for both a single spinodal curve which is located (see Figure 5) in a considerably lower temperature region, thereby suggesting significantly enhanced miscibility for these model blends at elevated pressures. The strong variation of UCST phase diagrams with pressure is also found in LCT computations for the corresponding A/B homopolymer blends and is a consequence of the rather large departure of ϵ_{11} from ϵ_{22}. Further implications of this large energetic asymmetry are presented in Figures 6−8, which are the counterparts for this system of Figures 2−4. The critical temperatures for the A_xB_{1-x}/A and A_xB_{1-x}/B systems become identical (see Figure 6) for $x^* = 0.4936$, which departs from the classic FH value of $x^* = 0.5$ somewhat more than the x^* for PS_x-$PMMA_{1-x}$/PS(PMMA) in Figure 2. The critical temperatures in Figure 6 are no longer linear functions of x for the compressible A_xB_{1-x}/A and A_xB_{1-x}/B mixtures. Figures 7 and 8 demonstrate how the larger $|\epsilon_{11} - \epsilon_{22}|$ induces greater deviations $\delta_T = |T_c - T_c^{(\infty)}|$ and $\delta_M = |M_c^{(\infty)} - M_c|$ from standard FH theory.

C. PS_xPVME_{1-x}/PS and PS_xPVME_{1-x}/PVME Blends. Before selecting the three van der Waals energies ϵ_{S-S}, $\epsilon_{VME-VME}$ and ϵ_{S-VME} describing the attractive interactions in PS_xPVME_{1-x}/PS and PS_x-$PVME_{1-x}$/PVME blends, it should be realized that both incompressible and compressible versions of FH type theories can not predict correct LCST phase diagrams

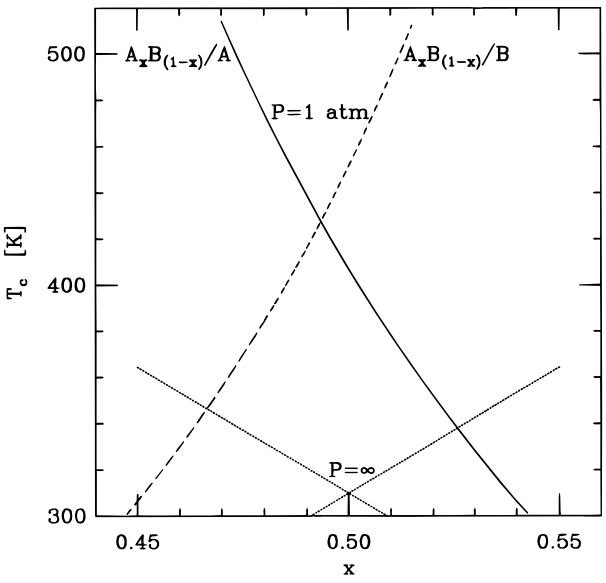

Figure 6. Variations of the critical temperature T_c for model UCST A_xB_{1-x}/A and A_xB_{1-x}/B systems (at $P = 1$ atm and $P = \infty$) with composition x.

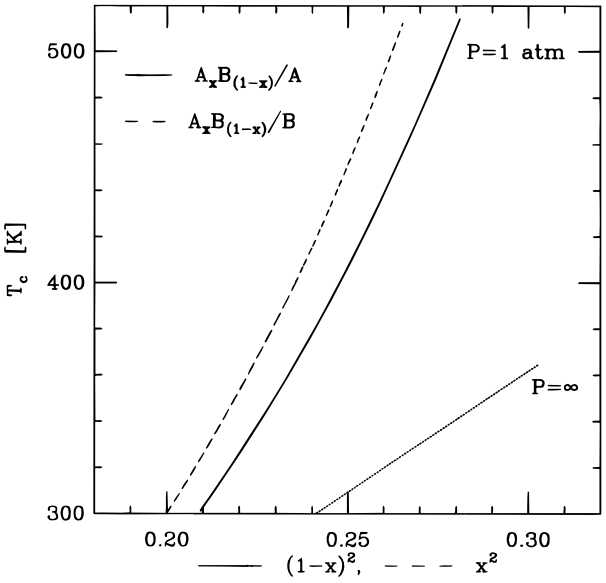

Figure 7. Same as Figure 4 but for model UCST A_xB_{1-x}/A and A_xB_{1-x}/B systems.

for these systems unless the interaction parameters χ_{ij} of eq 2.2a−c are modified. An example of such a modification is provided by eq 2.19a−c. The ratios $r_i \equiv N_2^{(i)}/M_i$, appearing in the entropic contributions χ_{ij}^{ent} of eq 2.19, are $r_1 = {}^{16}/_9$ and $r_2 = {}^5/_4$ for PS and PVME, respectively. While random copolymers of PS and PVME are not available, we expect that calculations for this system should be representative of general trends anticipated for random copolymers formed from monomers whose homopolymer blends display LCST phase diagrams. Before computing the LCST spinodals, we briefly discuss the choice of the three ϵ_{ij} and v_{cell}.

The self-interaction energy ϵ_{S-S} and the pure melt cell volume $v_{cell}^{(S)}$ are assumed to be the same as used for PS_xPMMA_{1-x}/PS(PMMA) mixtures, while the $\epsilon_{VME-VME}$ and $v_{cell}^{(VME)}$ are taken from the LCT fits[25] ($\epsilon_{VME-VME} = 0.59k_BT_o$ and $v_{cell}^{(VME)} = 90.4$ A^3) to pure component PVT data. The multiplication of the LCT $v_{cell}^{(VME)} = 22.60$ A^3 by a factor of 4 compensates for the difference (4 vs 1) in the occupancy indices for a vinyl methyl ether

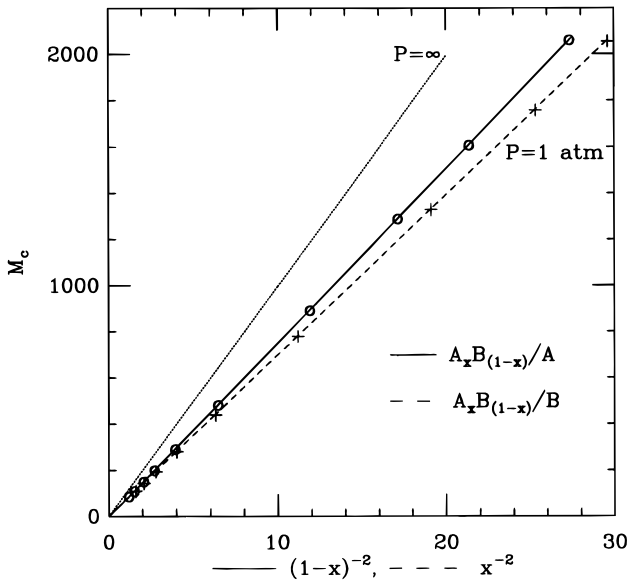

Figure 8. Same as Figure 5 but for model UCST A_xB_{1-x}/A and A_xB_{1-x}/B systems at $T = 400$ K.

monomer in the extended and standard lattice models, respectively. The cell volume for PS_xPVME_{1-x}/PS and PS_xPVME_{1-x}/PVME mixtures is determined from the combining rule of eq 3.1 with $v_{cell}^{(2)} = v_{cell}^{(S)}$ for the former system and $v_{cell}^{(2)} = v_{cell}^{(VME)}$ for the latter. The heterocontact interaction energy $\epsilon_{S-VME} = 0.606435k_BT_o$ is fit (by using eq 2.15 with the modified interaction parameters χ'_{ij}) to the experimental data of Han *et al.*[31] for PS/PVME spinodals. Note that the application of the Berthelot combining rule[24] for ϵ_{12} would yield $\epsilon_{S-VME} = 0.6048k_BT_o$. The latter deviates from the fitted value of $0.606435k_BT_o$ by less than 0.3% but produces a positive exchange energy ϵ and, therefore, an incorrect, UCST phase diagram.

In contrast to the PS_xPMMA_{1-x}/PS(PMMA) systems where computations indicate that an applied pressure diminishes miscibility, the random copolymer of PS and PVME mixes with pure PS or PVME much better at elevated pressures. Figure 9 illustrates this trend for the symmetric random copolymer $PS_{0.5}PVME_{0.5}$. At infinite pressures, the $PS_{0.5}PVME_{0.5}$/PS and $PS_{0.5}$-$PVME_{0.5}$/PVME blends (with corresponding polymerization indices) exhibit indistinguishable phase diagrams, but their computed P = 1 atm spinodal curves are slightly different. An increase in the percentage of PS in the PS_xPVME_{1-x} copolymer (or a decrease in the PVME content) facilitates the miscibility of the copolymer with PS and reduces its miscibility with PVME. This behavior is summarized in Figure 10 and arises because similar species always mix better. Equation of state effects shift the composition x^*, at which the critical temperatures of PS_xPVME_{1-x}/PS and PS_x-$PVME_{1-x}$/PVME are equal, from $x^* = 0.5$ for $P = \infty$ to $x^* = 0.49$ for $P = 1$ atm. The relative miscibilities of these two systems switch when $x - x^*$ changes its sign. The $P \rightarrow \infty$ limit critical temperatures in Figure 11 are no longer linear functions of $(1 - x)^2$ or x^2 as in standard FH theory because the modified interaction parameters χ'_{ij} now contain entropic contributions.

A series of computations has also been performed for another LCST random copolymer/homopolymer system with a larger disparity in ϵ_{11} and ϵ_{22}. This model system has the same $\epsilon_{11} = 0.62k_BT_o$ but a much less attractive $\epsilon_{22} = 0.5k_BT_o$. The heterocontact interaction energy ϵ_{12}

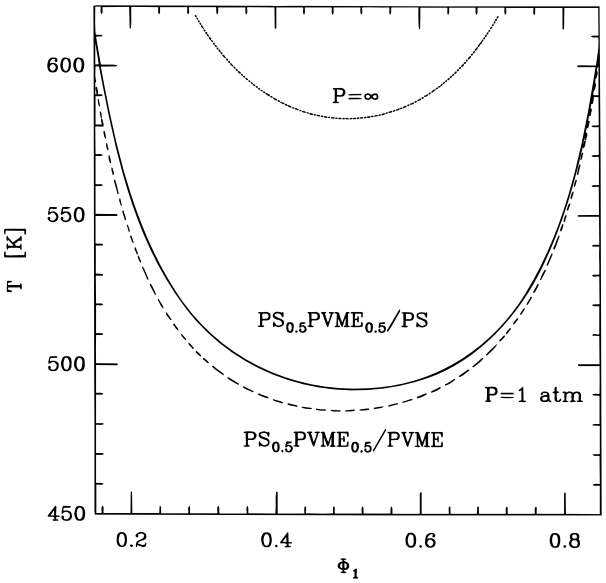

Figure 9. Spinodal curves for $PS_{0.5}PVME_{0.5}$/PS and $PS_{0.5}$-$PVME_{0.5}$/PVME blends at $P = 1$ atm and $P = \infty$. The curves are generated from the entropically modified compressible FH theory. The polymerization indices are taken as $M_1 = M_2 = 5000$ for this figure and Figures 10 and 11.

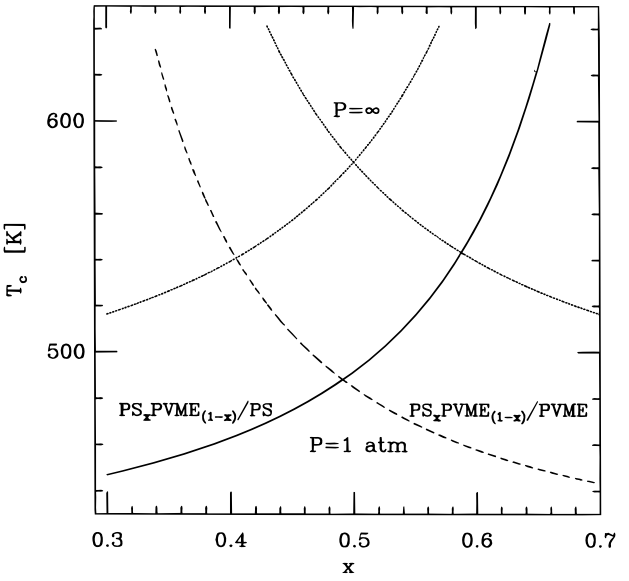

Figure 10. Same as Figure 2 but for PS_xPVME_{1-x}/PS and PS_x-$PVME_{1-x}$/PVME blends.

is chosen as $\epsilon = 0.561k_BT_o$ to yield the same PS/PVME exchange energy of $\epsilon = -0.00287k_BT_o$, and the cell volume is assumed to be identical to the v_{cell} for the PS_x-$PVME_{1-x}$/PS(PVME) mixtures. Hence, the basic difference lies in an enlarged $|\epsilon_{11} - \epsilon_{22}|$. The spinodal curves for these $A_{1/2}B_{1/2}$/A and $A_{1/2}B_{1/2}$/B blends (see Figure 12)-display quite different critical temperatures and critical compositions. Figure 12 does not depict the spinodal at $P \rightarrow \infty$ since computations for both systems produce complete miscibility in the incompressible limit. The miscibilities of these two systems also differ significantly over a wide range of x as displayed in Figure 13. The composition $x^* = 0.447$ (see Figure 13), at which the miscibilities become the same, varies from the symmetrical value of $x^* = 0.5$ by more than 10%, the highest shift of all systems considered. Figure 14 presents the critical temperature T_c as a function of $(1 - x)^2$ and x^2 for A_xB_{1-x}/A and A_xB_{1-x}/B, respectively, and emphasizes the huge influence of equation-of-state effects on the

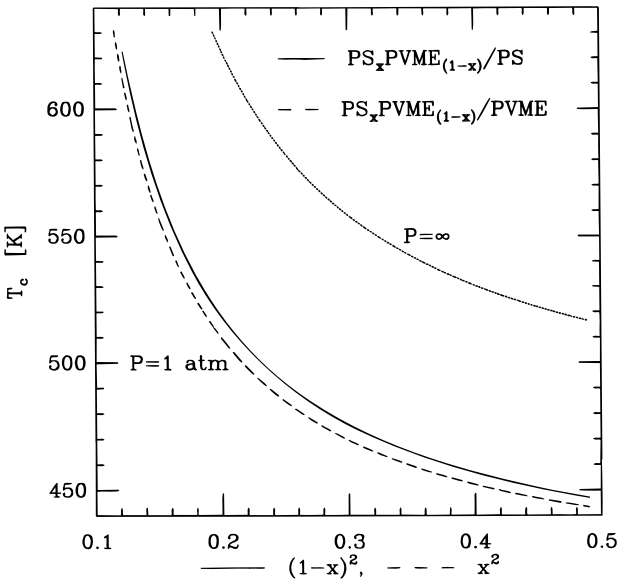

Figure 11. Same as Figure 3 but for PS_xPVME_{1-x}/PS and PS_x-$PVME_{1-x}$/PVME blends.

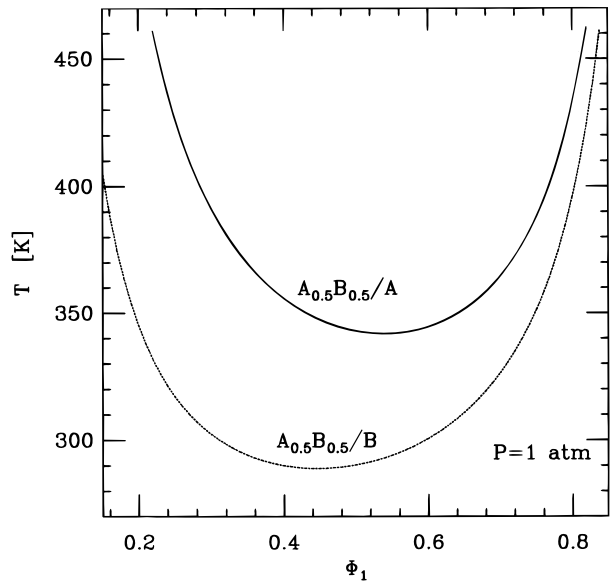

Figure 12. Spinodal curves for model LCST $A_{0.5}B_{0.5}$/A and $A_{0.5}B_{0.5}$/B blends at $P = 1$ atm. The curves are obtained from the entropically modified compressible FH theory (see eq 2.19a−c). The polymerization indices are chosen as $M_1 = M_2 = 1000$ and are also used for Figures 13 and 14.

phase behavior of the model LCST A_xB_{1-x}/A and A_xB_{1-x}/B random copolymer/homopolymer systems.

IV. Computations of Phase Diagrams for A_xB_{1-x}/A_yB_{1-y} Blend.

Experiments show that blends of two random copolymers with the same polymer species A and B but different compositions x and y display[15] varied patterns of miscibility windows. We examine this feature by considering $PS_xPMMA_{1-x}/PS_yPMMA_{1-y}$ and $PS_xPVME_{1-x}/PS_yPVME_{1-y}$ blends which are chosen to exemplify generic behaviors of upper and lower critical solution temperature systems, respectively. The spinodal curves are computed by using eq 2.14 with the interaction parameters $\{\chi'_{ij}\}$ defined by eq 2.8a−c. The attractive van der Waals energies $\{\epsilon_{ij}\}$ and the pure melt cell volumes $v_{cell}^{(S)}$, $v_{cell}^{(MMA)}$, and $v_{cell}^{(VME)}$ are taken from the fits described in section III, and the lattice coordination

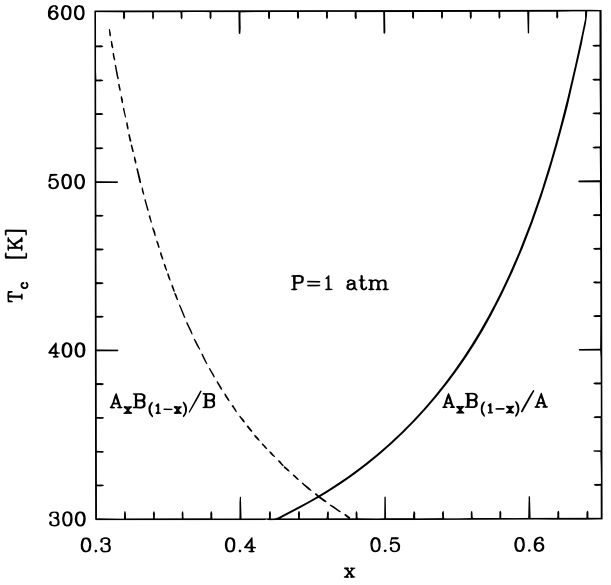

Figure 13. Same as Figure 6 but for model LCST A_xB_{1-x}/A and A_xB_{1-x}/B blends.

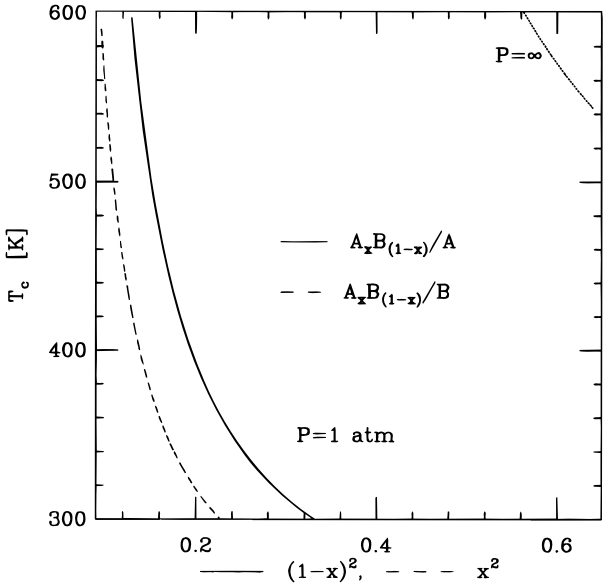

Figure 14. Same as Figure 7 but for model LCST A_xB_{1-x}/A and A_xB_{1-x}/B blends.

number is likewise $z = 6$. The entropic contributions to $\{\chi'_{ij}\}$ are evaluated from the LCT united atom structured monomer models[25,27] for PS and PVME, producing the geometrical coefficients $r_i = N_2^{(i)}/M_i$ as $r_{PS} = {}^{16}/_9$ and $r_{PVME} = {}^5/_4$, respectively. The cell volume v_{cell} is estimated from the combining rule (eq 3.1), with the random copolymer values $v_{cell}^{(1)}$ and $v_{cell}^{(2)}$ defined as in eq 3.2 by

$$v_{cell}^{(1)} = v_{cell}^{(A)}\, x + v_{cell}^{(B)}\,(1 - x)$$

and

$$v_{cell}^{(2)} = v_{cell}^{(A)}\, y + v_{cell}^{(B)}\,(1 - y)$$

where A ≡ S and B = MMA or VME. The computed phase diagrams at $P = 1$ atm exhibit a fair insensitivity to the choice of v_{cell}, whereas the $P = \infty$ spinodals are totally independent of v_{cell} by definition.

The phase diagrams for binary mixtures of two A-*co*-B random copolymers display shapes similar to those

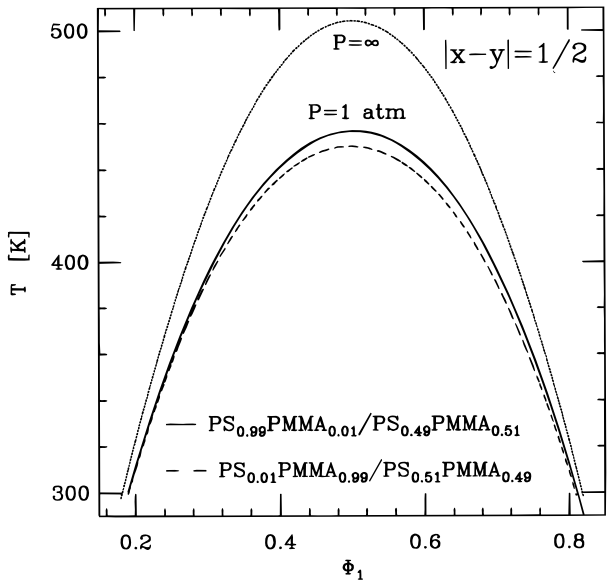

Figure 15. Spinodal curves for $PS_xPMMA_{1-x}/PS_yPMMA_{1-y}$ systems with varying x and y but the same $\delta = |x - y| = {}^1/_2$. The polymerization indices for two random copolymers are identical $M_1 = M_2 = 200$ and are also used for Figures 16 and 17.

computed for A-*co*-B/C = A,B random copolymer/homopolymer blends. Figure 15 depicts an example of spinodal curves for $PS_xPMMA_{1-x}/PS_yPMMA_{1-y}$ mixtures with variable x and y but with fixed $\delta \equiv |x - y| = {}^1/_2$. While classic FH theory predicts that these blends yield identical phase diagrams, which coincide with those predicted for $PS_{0.5}PMMA_{0.5}$/PS and $PS_{0.5}PMMA_{0.5}$/PMMA systems with the corresponding molecular weights for both components, the compressible FH type approach admits a small variation of the phase diagrams with $(x + y)$ in the region of high temperatures. Figure 15 presents the $PS_{0.01}PMMA_{0.99}/PS_{0.51}PMMA_{0.49}$ blend as more miscible than $PS_{0.99}PMMA_{0.01}/PS_{0.49}$-$PMMA_{0.51}$, a feature already evident from Figure 2 which illustrates the behavior of PS_xPMMA_{1-x}/PS and PS_xPMMA_{1-x}/PMMA systems, which are limits of PS_x-$PMMA_{1-x}/PS_yPMMA_{1-y}$ blends for $x \to 0$ and $y \to 0$. Figure 15 displays the miscibility of two A-*co*-B random copolymers as depending on their averaged composition $s = (x + y)/2$, in accord with many experiments.[16–18] This feature is even more apparent in Figure 16, which presents the variation with $\delta^2 = |x - y|^2$ of the critical temperature for the $PS_{0.99}PMMA_{0.01}/PS_yPMMA_{1-y}$ and $PS_{0.01}PMMA_{0.99}/PS_yPMMA_{1-y}$ mixtures. As δ grows, the miscibility disparity increases for these two systems. The inset to Figure 16 illustrates the slight dependence of T_c on the averaged composition $s = (x + y)/2$ for fixed $\delta = 0.54$. On the other hand, standard FH theory does not distinguish between $PS_xPMMA_{1-x}/PS_yPMMA_{1-y}$ systems with the same $\delta = |x - y|$. The incompressible FH theory critical temperature in Figure 16 is linear in δ^2, and its slope coincides with the slope of T_c versus $(1 - x)^2$ (or x^2) for PS_xPMMA_{1-x}/PS (or PS_xPMMA_{1-x}/PMMA) systems with corresponding molecular weights.

Miscibility boundaries for a mixture of two random copolymers A_xB_{1-x} and A_yB_{1-y} at a given temperature T are usually presented as a plot of y vs x. Figure 17 provides an example of this isothermal phase diagram for $PS_xPMMA_{1-x}/PS_yPMMA_{1-y}$ blends with equal amounts of both random copolymers ($\Phi_1 = \Phi_2 = 0.5$). The solid lines in Figure 17 designate the miscibility boundary generated from the compressible FH type

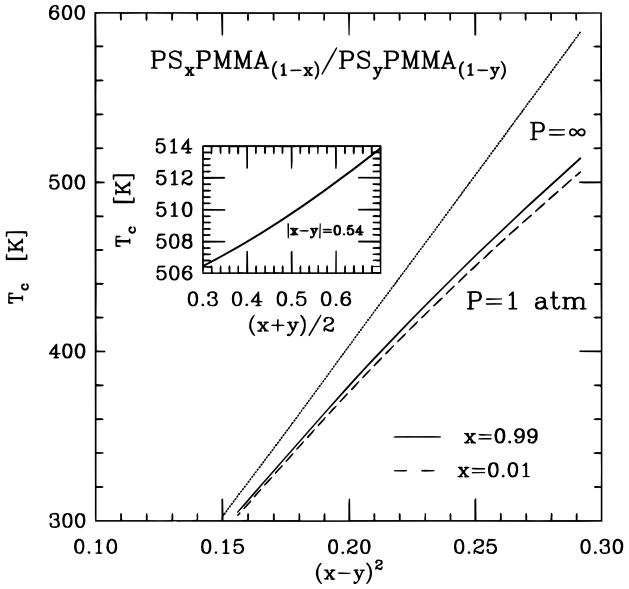

Figure 16. Critical temperature T_c of PS_xPMMA_{1-x}/PS_y-$PMMA_{1-y}$ blends as a function of $(x - y)^2$. The inset illustrates the variation of T_c with the average composition $s = (x + y)/2$ for the $P = 1$ atm systems with constant $\delta = |x - y|$.

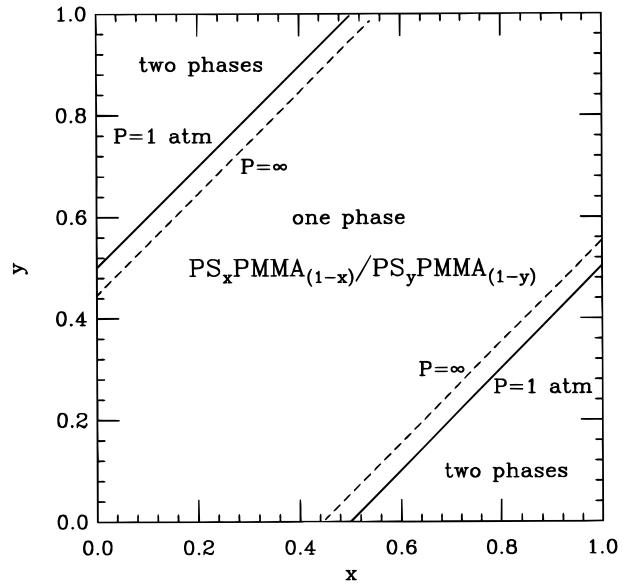

Figure 17. Isothermal phase diagram of PS_xPMMA_{1-x}/PS_y-$PMMA_{1-y}$ blends at $T = 450$ K. The volume fractions and polymerization indices of two random copolymers are symmetrical; i.e., $\Phi_1 = \Phi_2 = 0.5$ and $M_1 = M_2 = 200$.

theory, while dashed lines correspond to the standard FH theory, which underestimates the miscibility as it generally does for UCST systems. The region between the parallel lines in Figure 17 corresponds to a homogeneous one-phase system, whereas the regions outside these lines designate two-phase mixtures. Neither theory predicts miscibility patterns similar to those featuring bulges as found by Chai *et al.*[15] for chlorinated polyethylene random copolymer blends.

Introducing a greater disparity in the self-interaction energies ϵ_{11} and ϵ_{22} (by choosing $\epsilon_{11} = 0.6k_BT_o$ and $\epsilon_{22} = 0.5k_BT_o$) and assuming $\epsilon_{12} = (\epsilon_{11}\epsilon_{22})^{1/2}$ as the geometrical mean of ϵ_{11} and ϵ_{22} lead to larger differences in the miscibilities of A_xB_{1-x}/A_yB_{1-y} mixtures with the same $|x - y|$ but different $x + y$. Figure 18 shows how the critical temperatures T_c for the $A_{0.99}B_{0.01}/A_yB_{1-y}$ and $A_{0.01}B_{0.99}/A_yB_{1-y}$ systems change with $\delta^2 = |x - y|^2$, and the inset exhibits the variation of T_c at fixed $\delta = 0.5$ as

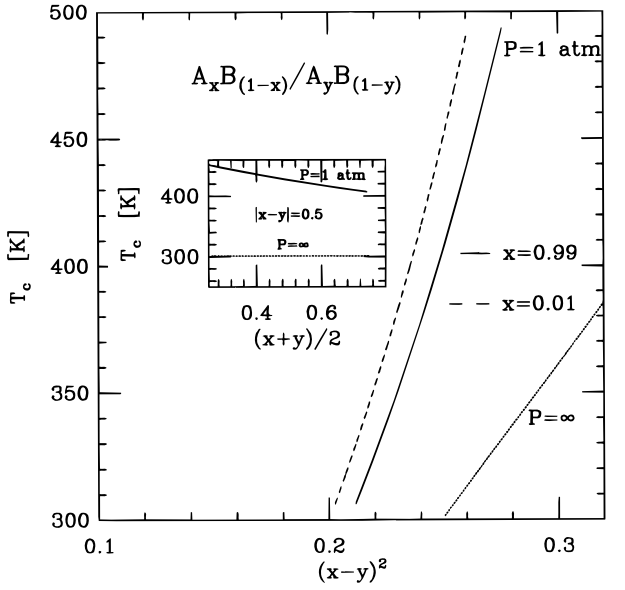

Figure 18. Variations of the critical temperature T_c for model UCST A_xB_{1-x}/A_yB_{1-y} blends with $(x - y)^2$. Only classic FH theory produces a linear behavior of T_c with $(x - y)^2$. The polymerization indices are chosen as $M_1 = M_2 = 300$. The inset illustrates the dependence of T_c on the averaged composition $s = (x + y)/2$, as predicted by the compressible extension of FH theory.

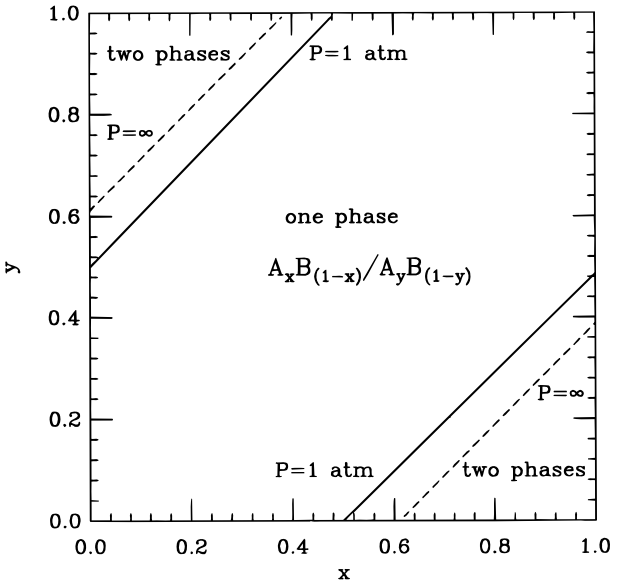

Figure 19. Isothermal phase diagram of model UCST A_xB_x/A_yB_{1-y} blends at $T = 450$ K. The volume fractions Φ_1 and Φ_2 of the two random copolymers are equal as are the polymerization indices ($M_1 = M_2 = 300$).

functions of the averaged composition $s = (x + y)/2$. The dependence of T_c on $s = (x + y)/2$ is now much more pronounced than for the $PS_xPMMA_{1-x}/PS_yPMMS_{1-y}$ blends, where the self-interaction energies ϵ_{S-S} and $\epsilon_{MMA-MMA}$ are more similar. The horizontal line in the inset represents the prediction of incompressible FH theory. The isothermal phase diagram for the A_xB_{1-x}/A_yB_{1-y} mixture at a pressure of 1 atm (see Figure 19) is similar but displaced from that in Figure 17. The only significant change concerns the influence of pressure, which unexpectedly enhances the miscibility, probably because of the presence of more disparate ϵ_{11} and ϵ_{22}.

Computations for the LCST $PS_xPVME_{1-x}/PS_yPVME_{1-y}$ mixtures do not exhibit additional features. The varia-

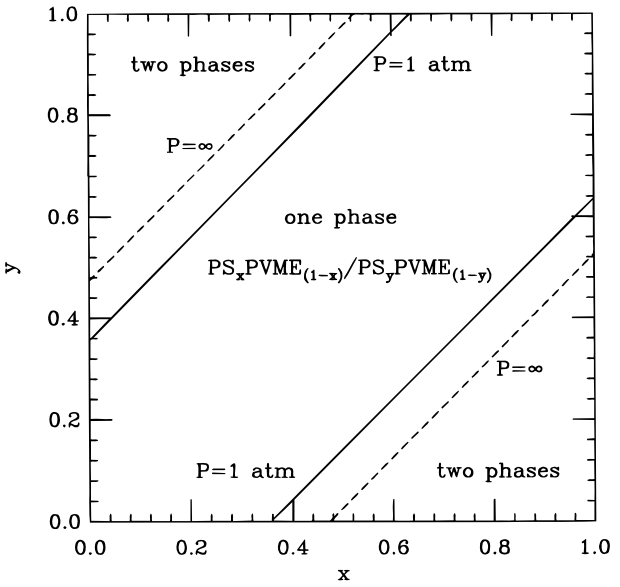

Figure 20. Same as Figure 19 but for LCST PS$_x$PVME$_{1-x}$/PS$_y$PVME$_{1-y}$ blends at $T = 600$ K and with $M_1 = M_2 = 5000$.

tion of the critical temperatures T_c with δ^2 for given x resembles the changes of T_c with $(1 - x)^2$ and x^2 for PS$_x$PVME$_{1-x}$/PS and PS$_x$PVME$_{1-x}$/PVME systems, respectively. Figure 20 depicts the isothermal phase diagram at $T = 600$ K and suggests that the modification of FH type theories to describe LCST random copolymer system cannot produce nonlinear miscibility boundaries.

V. Discussion

The phase behavior of binary random copolymer blends is analyzed within the extension to compressible systems of random copolymer FH type theories. Compressibility introduces familiar "equation-of-state effects" associated with density differences between the blend components but also with features driven by energetic asymmetries as follows: The distribution of excess volume is governed in our model by the magnitudes of the interaction energies $\{\epsilon_{ij}\}$ because the creation of voids in an otherwise incompressible binary blend requires the removal of polymer-polymer contacts, a removal that incurs an energy cost of ϵ_{11}, ϵ_{22}, or ϵ_{12}, depending upon whether the broken contact is between segments of component 1 or of component 2 or between segments of differing components, respectively. Consequently, one main focus in this study is placed on understanding the influence of energetic asymmetries between the two blend species. Another focus concerns the pressure dependence of random copolymer miscibilities. The analysis includes UCST and LCST A$_x$B$_{1-x}$/A,B random copolymer/homopolymer mixtures, as well as UCST and LCST blends of two random copolymers of the same species but different compositions. The LCST systems are described by introducing a simple model of the noncombinatorial entropy based on the LCT theory for homopolymer blends. This model is designed to illustrate an alternative mechanism to that traditionally invoked as following from "equation-of-state" effects[12] or from a cancellation between enthalpic and "equation-of-state" terms.[12,21] More precisely, the equation of state mechanism focuses on differences in volumetric expansion coefficients between the two blend components and on the resultant unfavorable entropy of mixing that increases upon the heating of the system.[21] The simple model introduced here considers the strong influence of the noncombinatorial entropy associated with the mixing of polymer chains whose monomers have differing sizes and shapes.[27]

While PS/PMMA homopolymer blends are found to be fairly immiscible, mixtures of a PS$_x$PMMA$_{1-x}$ random copolymer and pure PS or PMMA exhibit improved miscibility. This behavior accords with physical intuition which anticipates that similar polymer species should mix better. Thus, the greater similarity of the random copolymer A$_x$B$_{1-x}$ to a homopolymer of pure species A (or B) than that between homopolymers A and B promotes the improved miscibility for the former. The same argument explains an increase of the PS percentage in the PS$_x$PMMA$_{1-x}$ random copolymer as enhancing its miscibility with PS and as weakening its miscibility with PMMA.

Classic incompressible FH theory relates the above miscibility disparities only to differences in the effective interaction parameters χ_{eff}. A binary PS/PMMA blend with a positive (unfavorable) exchange energy $\epsilon = \epsilon_{S-S} + \epsilon_{MMA-MMA} - 2\epsilon_{S-MMA}$ has the S-MMA contacts less favorable than the like S−S and MMA−MMA contacts. This positive ϵ translates into a positive binary blend FH interaction parameter $\chi_{AB} = \epsilon z/(2k_BT)$. The effective interaction parameters for the random copolymer PS$_x$-PMMA$_{1-x}$/PS and PS$_x$PMMA$_{1-x}$/PMMA blends also depends on the composition x through

$$\chi_{AB/A} = (1 - x)^2\chi_{AB} \tag{5.1}$$

and

$$\chi_{AB/B} = x^2\chi_{AB} \tag{5.2}$$

respectively. Since the composition lies in the range $0 \le x \le 1$, both $\chi_{AB/A}$ and $\chi_{AB/B}$ are smaller than χ_{AB}, implying a lower free energy for the blend and, hence, a higher miscibility for both random copolymer mixtures.

Generally, a binary blend with a positive exchange energy ϵ separates upon cooling, which, in turn, indicates that the blend critical temperature T_c and blend miscibility move in opposite directions with various changes in compositions, etc. Consequently, our computations predict that the T_c of a PS$_x$PMMA$_{1-x}$/PS blend declines, while the T_c of a PS$_x$PMMA$_{1-x}$/PMMA system grows with increasing PS content in the random copolymer PS$_x$PMMA$_{1-x}$. Figure 2 demonstrates the existence of an $x = x^* \neq 0.5$ for which the critical temperatures of these two systems are equal. Incompressible FH theory always yields $x^* = 0.5$, and this composition changes only slightly upon introduction of equation-of-state effects into incompressible FH type treatments. In contrast, the shifts in T_c between the incompressible ($T_c^{(\infty)}$) and compressible theories are significant, indicating a potentially large pressure dependence because the incompressible theory represents a high pressure limit of the compressible treatment. Model UCST A$_x$B$_{1-x}$/A,B blends with more disparate self-interaction energies ϵ_{AA} and ϵ_{BB} than ϵ_{S-S} and $\epsilon_{MMA-MMA}$ display x^* as departing more from 0.5 and yield larger differences $|T_c - T_c^{(\infty)}|$ due to compressibility effects. Usually, the incompressible FH theory overestimates the critical temperature (see for instance Figures 1−3), but the computations in Figures 5−7 indicate that the reverse behavior is also possible. In either case $T_c^{(\infty)}$ is a linear function of x^2 or $(1 - x)^2$. In spite of obvious limitations, both classic and compressible FH theories

explain some qualitative trends in the asymmetric miscibilities observed by Russell *et al.*[19] for PS_xPMMA_{1-x}/PS and PS_xPMMA_{1-x}/PMMA blends.

One main deficiency of FH type approaches (both compressible and incompressible) lies in their entire inadequacy for describing the behavior of blends with negative exchange energy ϵ.[32] The systems are predicted to be completely miscible at all temperatures and for arbitrary molecular weights. However, experiments for some such systems demonstrate the occurrence of a phase separation upon heating and a LCST phase diagram. The addition of a temperature-independent, i.e., entropic, contribution χ_{ij}^{ent} to each of the interaction parameters χ_{ij} (see eq 2.19a−c) is one simple remedy enabling the theoretical treatment of random copolymer LCST systems, a situation illustrated for PS_x-$PVME_{1-x}$/PS and PS_xPVME_{1-x}/PVME mixtures. The entropic contributions χ_{ij}^{ent} must be sufficiently large to overcome the negative energetic portion of χ_{eff}, and the χ_{ij}^{ent} are assumed in our model, for simplicity, to depend on the composition x in the same fashion as the original unmodified χ_{ij} parameters in eqs 2.2a−c and 2.8a−c. This assumption ensures consistency with the known behavior for binary homopolymer blends that emerges[27] from the LCT in the limits of $T, P \to \infty$ and $x \to 0$ (or $x \to 1$). This model for χ_{ij}^{ent} is based on LCT treatments for homopolymer blends and therefore requires *no additional parameters*. However, the simple model ignores potentially crucial sequence dependent contributions which will be analyzed in a future work[9] within a full LCT of random copolymer blends.

The computed miscibilities of PS_xPVME_{1-x}/PS and PS_xPVME_{1-x}/PVME mixtures likewise exceed the very high compatibility of PS/PVME blends that arise because of a negative exchange energy $\epsilon = \epsilon_{S-S} + \epsilon_{VME-VME} - 2\epsilon_{S-VME}$. Again, a high PS content in the PS_xPVME_{1-x} random copolymer facilitates its mixing with PS and worsens the miscibility with PVME. The incompressible limit of our entropically modified FH theory already provides insights into the above trends. The effective interaction parameter χ_{AB} for PS/PVME blends becomes positive owing to the presence of the entropic contributions to χ_{ij}. Equations 5.1 and 5.2 for the dependence on x of $\chi_{AB/A}$ and $\chi_{AB/B}$ for A_xB_{1-x}/A and A_xB_{1-x}/B mixtures, respectively, maintain their forms for the LCST random copolymer/homopolymer systems. Hence, the inequalities $\chi_{AB/A} < \chi_{AB}$ and $\chi_{AB/B} < \chi_{AB}$, etc., remain and produce the obvious implications.

Computations for blends of a random copolymer PS_xPVME_{1-x} with pure PS or PVME, however, display a different dependence of the critical temperature T_c on composition x than do the PS_xPMMA_{1-x}/PS,PMMA systems. When the PS percentage in the PS_xPVME_{1-x} random copolymer increases, the T_c of the PS_xPVME_{1-x}/PS mixture grows, and the T_c for the PS_xPVME_{1-x}/PVME blend diminishes, opposite to the behavior found for PS_xPMMA_{1-x}/PS and PS_xPMMA_{1-x}/PMMA mixtures. The composition x^*, where the critical temperatures for PS_xPVME_{1-x}/PS and PS_xPVME_{1-x}/PVME systems become equal, varies likewise slightly (by about 2%) from the 0.5 that emerges from incompressible FH theory and that is unaltered when the incompressible theory is entropically modified according to eq 2.20a−c. Lifting the incompressibility assumption leads, however, to a significant decline of the critical temperatures for both PS_xPVME_{1-x}/PS and PS_xPVME_{1-x}/PVME mixtures (see Figures 10 and 11), as well as for other model LCST A_xB_{1-x}/A and A_xB_{1-x}/B systems (see Figures 12 and 13). This decline of T_c is symptomatic of a large variation of T_c with pressure.

Computations for blends of two random copolymers of the same species A and B but different compositions x and y demonstrate that blend miscibility depends not only on the composition difference $\delta = |x - y|$ but also on the averaged composition $s = (x + y)/2$, a feature observed[16−18] in many experiments. The dependence on $(x + y)$ arises in the calculations from equation-of-state effects since the dependence is absent in computations for incompressible systems. Both PS_xPMMA_{1-x}/PS_y-$PMMA_{1-y}$ and PS_xPVME_{1-x}/PS_yPVME_{1-y} blends exhibit improved miscibility with increased δ. The isothermal phase boundaries (presented as a plot of y versus x) are determined by a pair of straight parallel lines. Both compressible versions of FH theory (without or with entropic contributions χ'^{ent}_{ij} of eq 2.20a−c) cannot predict nonlinear shapes of miscibility windows, a feature already well-known for classic incompressible FH random copolymer theory where the effective interaction parameter $\chi_{AB/AB}$ for blends of two A-*co*-B random copolymers varies as $\chi_{AB/AB} = (x - y)^2\chi_{AB}$. Figures 17, 19, and 20 indicate that compressibility effects do not qualitatively change the linear shapes of the miscibility boundaries. Such an alteration may arise from sequence dependent contributions to the free energy, as postulated by Chai *et al.*[15] A full molecular based theory is, however, necessary to verify this hypothesis without ascribing to χ_{eff} an ad hoc monomer sequence dependence with a myriad of adjustable six-monomer interaction parameters. Such a molecular theory is under development[9] using the extension to random copolymers of the LCT.

Acknowledgment. We are grateful to Tom Russell for supplying his data prior to publication. This research is supported, in part, by Grant No. DAAG55-97-1-0162 from ARO.

References and Notes

(1) Kambour, R. P.; Bendler, J. T.; Bopp, R. C. *Macromolecules* **1983**, *16*, 753.
(2) Roe, R. J.; Rigby, D. *Adv. Pol. Sci.* **1987**, *82*, 103.
(3) Huh, W.; Karasz, F. E. *Macromolecules* **1992**, *25*, 1057.
(4) ten Brinke, G.; Karasz, F. E.; MacKnight, W. J. *Macromolecules* **1983**, *16*, 1827.
(5) Roe, R. J.; Zim, W. C. *Macromolecules* **1980**, *13*, 1221; Paul, D. R., Barlow, J. W. *Polymer* **1984**, *25*, 487.
(6) Balazs, A. C.; Sanchez, I. R.; Epstein, I. R.; Karasz, F. E.; MacKnight, W. J. *Macromolecules* **1985**, *18*, 2188.
(7) Dudowicz, J.; Freed, K. F. *Macromolecules* **1996**, *29*, 7826.
(8) Dudowicz, J.; Freed, K. F. *Macromolecules* **1991**, *24*, 5076.
(9) Freed, K. F.; Dudowicz, J. To be published.
(10) Dudowicz, J.; Freed, K. F. *Macromolecules* **1990**, *23*, 1519.
(11) Flory, P. J.; Orwoll, R. A.; Vrij, A. *J. Am. Chem. Soc.* **1964**, *86*, 3507, 3515.
(12) Sanchez, I. C.; Lacombe, R. H. *Macromolecules* **1978**, *11*, 1145.
(13) Paul, D. R. *Pure & Appl. Chem.* **1995**, *67*, 977. Kim, C. K.; Paul, D. R. *Polymer* **1992**, *33*, 1631, 2089, 4929, 4941. Callaghan, T. A.; Paul, D. R. *J. Polym. Sci. B Polym. Phys.* **1994**, *32*, 1813, 1847. Callaghan, T. A.; Takakuwa, K.; Paul, D. R.; Padwa, A. R. *Polymer* **1993**, *34*, 3797.
(14) Gan, P. P.; Paul, D. R. *Polymer* **1994**, *35*, 3513; *J. Appl. Polym. Sci.* **1994**, *54*, 317. Gan, P. P.; Paul, D. R.; Padwa, A. R. *Polymer* **1994**, *35*, 1487.
(15) Chai, Z.; Sun, R.; Karasz, F. E. *Macromolecules* **1992**, *25*, 6113; **1995**, *28*, 2297.
(16) Krishnamoorti, R.; Graessley, W. W.; Balsara, N. P.; Lohse, D. J. *Macromolecules* **1994**, *27*, 3073. Graessley, W. W.; Krishnamoorti, R.; Balsara, N. P.; Butera, R. J.; Fetters, L. J.; Lohse, D. J.; Schulz, D. N.; Sisano, J. A. *Macromolecules* **1994**, *27*, 2574, 3896. Graessley, W. W.; Krishnamoorti, R.; Reichart, G. C.; Balsara, N. P.; Fetters, L. J.; Lohse, D. J. *Macromolecules* **1995**, *28*, 1260.

(17) Rhee, J.; Crist, B. *Macromolecules* **1991**, *24*, 5663. Nicholson, J. C.; Finerman, T. M.; Crist, B. *Polymer* **1990**, *31*, 2287.
(18) Scheffold, F.; Eiser, E.; Butkowski, A.; Steiner, U.; Klein, J.; Fetters, L. J. *J. Chem. Phys.* **1996**, *104*, 8786.
(19) Russell, T. P. Private communication. Kulasekere, R.; Kaiser, H.; Ankner, J. F.; Russell, T. P.; Brown, H. R.; Hawker, C. J.; Mayes, A. M. *Macromolecules* **1996**, *29*, 5493.
(20) Winey, K. I.; Berba, M. L.; Galvin, M. E. *Macromolecules* **1996**, *29*, 2868.
(21) Patterson, D. *Macromolecules* **1969**, *2*, 672.
(22) Dudowicz, J.; Freed, K. F. *J. Chem. Phys.* **1994**, *100*, 4653.
(23) Lupis, C. H. P.; *Chemical Thermodynamics of Materials*; P T R Prentice Hall: Englewood Cliffs, NJ, 1983.
(24) Rowlinson, J. S.; Swinton, F. L. *Liquids* and *Liquid Mixtures*; 3rd. ed.; Butterworths: London, 1982.
(25) Dudowicz, J.; Freed, K. F. *Macromolecules* **1995**, *28*, 6625.
(26) Freed, K. F.; Dudowicz, J. *Trends Polym. Sci.* **1995**, *3*, 248.
(27) Dudowicz, J.; Freed, K. F. *Macromolecules* **1991**, *24*, 5112.
(28) Dudowicz, J.; Freed, K. F. *Macromolecules* **1996**, *29*, 8960. Freed, K. F.; Dudowicz, J. *Macromolecules* **1996**, *29*, 625.
(29) Hamada, F.; Shiomi, T.; Fujisawa, K.; Nakajima, A. *Macromolecules* **1980**, *13*, 729. Shiomi, T.; Fujisawa, K.; Hamada, F.; Nakajima, A. *J. Chem. Soc., Faraday Trans. 1* **1980**, *76*, 885. Fujisawa, K.; Shiomi, T.; Hamada, F.; Nakajima, A. *Polym. Bull.* **1980**, *3*, 261.
(30) Callaghan, T. A.; Paul, D. R. *Macromolecules* **1993**, *26*, 2439.
(31) Han, C. C.; Bauer, B. J.; Clark, J. C.; Muroga, Y.; Matsushita, Y.; Okada, M.; Tran-cong, Q.; Chang, T.; Sanchez, I. C. *Polymer* **1988**, *29*, 2002.
(32) Sanchez-Lacombe theory accounts for a LCST phase behavior due to the presence of three parameters P^*, T^*, and v^* for each binary blend component and due to the use of specific combining rules for P^*, T^*, and v^* for mixtures. A similar type of argument applies to Flory−Orwoll−Vrij theory.

MA9702105